Talanta 252 (2023) 123868

Contents lists available at ScienceDirect

Talanta

journal homepage: www.elsevier.com/locate/talanta

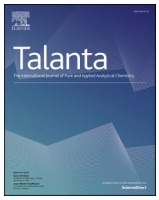

Liquid-liquid microextraction with hydrophobic deep eutectic solvent followed by magnetic phase separation for preconcentration of antibiotics

Aleksei Pochivalov [a,*], Ksenia Cherkashina [a], Andrey Sudarkin [a], Mikhail Osmolowsky [a], Olga Osmolovskaya [a], Firuza Krekhova [a], Lawrence Nugbienyo [b], Andrey Bulatov [a]

[a] Department of Analytical Chemistry, Institute of Chemistry, Saint-Petersburg University, Saint-Petersburg State University, 7/9 Universitetskaya Nab., Saint-Petersburg, 199034, Russia

[b] Faculty of Applied Sciences, Accra Technical University, GA, 106-2535, Accra, Ghana

ARTICLE INFO

Keywords:
liquid-Liquid microextraction
Magnetic phase separation
Hydrophobic deep eutectic solvent
Magnetic nanoparticles
HPLC-FLD
Fluoroquinolones

ABSTRACT

This study describes a miniaturized approach for liquid-liquid microextraction based on mass transfer into low volume of deep eutectic solvent and magnetic phase separation, using specially produced magnetic chromium dioxide nanoparticles with a hydrophobic surface layer of fatty acids. The nanoparticles modified with fatty acid helped to recover low volumes of viscous hydrophobic deep eutectic solvent-based extract reproducibly and easily (up to 10 μL) in a microextraction procedure with the application of magnetic forces. It was demonstrated that the collector properties depend on nanoparticles' surface and magnetic characteristics. The developed approach was implemented for the separation and preconcentration of trace fluoroquinolone antibiotics from environmental waters prior to their determination by high-performance liquid chromatography with fluorometric detection as a model analytical task. The limits of detection, calculated from a blank test based on 3σ, were 0.01 μg L^{-1} for ofloxacin, 0.02 μg L^{-1} for lomefloxacin and fleroxacin, and 0.04 μg L^{-1} for norfloxacin. The procedure provides significant solvent reduction and high enrichment factors. The approach is green, which is proved by the analytical eco-scale assessment tool with the total score equal to 85 out of 100.

1. Introduction

Deep eutectic solvents (DESs) have attracted the attention of researchers in several areas of science and technology in recent years due to various reasons. These solvents are considered as a green alternative to conventional organic solvents due to their beneficial characteristics, such as high thermal stability, negligible vapor pressure, non-flammability, and miscibility with different solvents [1]. Usually, precursors used for the preparation of DESs are inexpensive, non-toxic [2,3], and often biodegradable [4]. DESs are widely used for organic and inorganic synthesis [5,6], in electrochemical deposition of metals for obtaining composite materials [7], as electrolytes for solar cells [8], as modifiers of various materials (magnetic nanoparticles (MNPs)) [9], sensors [10], and quantum dots [11]), and for liquid-liquid microextraction (LLME) [12,13].

Recently, hydrophobic DESs were found to be efficient for separation and preconcentration of various organic compounds from aqueous matrices [14–19]. The first hydrophobic DESs were formed based on interaction between carboxylic acids as hydrogen bond donors and quaternary ammonium salts as hydrogen bond acceptors [20]. Later, it was shown that DESs based on carboxylic acids and tetrabutylammonium bromide were unstable in aqueous phase due to the dissolution and dissociation of the quaternary ammonium salt in water [13]. Meanwhile, hydrophobic DESs based on carboxylic acids and terpenoids are stable in a wide range of aqueous samples, from which target analytes can selectively be separated into the DESs with high enrichment factors (EFs) [21,22].

However, LLME procedures based on hydrophobic DESs have several drawbacks; as the hydrophobic precursors (such as terpenoids and fatty acids) of these DESs are incompatible with chromatographic separation and detection in water-polar organic solvent mixtures. Usually, DESs are diluted by polar solvents before used in chemical analysis [23,24], including back extraction of target analytes into aqueous phase [25]. Other drawbacks of DESs are their relatively high viscosity and low density, which makes their collection in micro-liter amounts difficult and irreproducible. Several approaches for the elimination of these

* Corresponding author.
E-mail addresses: alexpochival@bk.ru, a.pochivalov@spbu.ru (A. Pochivalov).

https://doi.org/10.1016/j.talanta.2022.123868
Received 2 July 2022; Received in revised form 17 August 2022; Accepted 18 August 2022
Available online 24 August 2022

drawbacks are presented in literature; one of them is based on the solidification of floating organic droplet [26–28], by which the extract phase could solidify in ice bath or refrigerator for easy collection. In this case, the extraction solvent (DES) with low density and a particular freezing point floats above the aqueous phase and solidifies at low temperature. The extract phase is then analyzed after melting [29]. DES-based ferrofluids, known to be stable and uniform solid-liquid composite materials consisting of magnetic nanoparticles (MNPs) suspended in base fluids, have also been used as extraction solvents [30]. These ferrofluids are typically prepared by coating nanoparticles with already-prepared DESs. After an aqueous sample is mixed with a DES-based ferrofluid, the obtained extract phase can be separated by an external magnetic field without centrifugation. Since DES-based ferrofluids are not suitable solvents for analytical instrumentation, a back extraction step is typically required before analysis.

In this work, a new approach is suggested for miniaturized LLME based on mass transfer into low volume of DES followed by magnetic phase separation, using MNPs. The work demonstrates the use of MNPs as an extract phase collector, which allows significant reduction in DES consumption (down to 10 μL) without decrease in reproducibility. For the first time, MNPs have been used to reproducibly and easily recover microliter amounts of viscous hydrophobic DES-based extracts in an LLME procedure by the application of magnetic forces. Previously reported study [31] devoted to the topic involved simultaneous addition of MNPs and hydrophilic DES in a relatively large volume (200 μL) to the sample followed by solid-phase extraction and liquid-liquid extraction proceeding at the same time.

The developed approach was implemented for the separation and preconcentration of fluoroquinolones (ofloxacin, lomefloxacin, fleroxacin, and norfloxacin) from environmental water samples prior to their determination by high-performance liquid chromatography with fluorometric detection (HPLC-FLD) as an analytical task model. Fluoroquinolones are synthetic broad-spectrum antibiotics used in human, as well as veterinary medicine for the treatment of various bacterial infections [32]. Fluoroquinolones consumed by humans or livestock by oral or parenteral means of administration are subsequently excreted into the environment, most commonly, in active form [33]. The entry of these drugs into the environment, especially, into water systems, leads to the development of antibiotic resistant bacteria. There is also evidence of genotoxicity of fluoroquinolones [34], which makes their presence in the environment, even in trace amounts, extremely dangerous. Thus, the determination of fluoroquinolones in environmental water samples is of great importance for environmental monitoring.

2. Experimental

2.1. Reagents and solutions

All chemicals and reagents were of analytical grade. Ultra-pure water from Millipore Milli-Q RG (Millipore, USA) was used. Ofloxacin, lomefloxacin, fleroxacin, norfloxacin, thymol, hexane, Na_2HPO_4 and NaH_2PO_4, hexanoic, heptanoic, octanoic and nonanoic acids were purchased from Sigma-Aldrich (Germany). Methanol was purchased from J. T. Baker Chemical Company (USA). CrO_3, Cr_2O_3, and Fe_2O_3, used for magnetic nanoparticles production, were purchased from Nevareactiv (Russia). SbC_2O_4OH was synthesized as described in literature [35].

Stock solutions of analytes (1.0 g L^{-1}) were prepared by dissolving the corresponding amounts of substances in 0.01 mol L^{-1} NaOH. The stock solutions were stored in a dark place at 5 °C and used within 1 month. Working solutions of fluoroquinolones were prepared immediately before the experiments by dilution of the stock solutions with ultra-pure water. Phosphate buffer solution (pH 6.4) was prepared by mixing of 0.05 mol L^{-1} Na_2HPO_4 and 0.05 mol L^{-1} NaH_2PO_4 (255:745, v/v), and adjusted with 1 mol L^{-1} NaOH.

2.2. Apparatus

Chromatographic separation was carried out, using LC-20 Prominence liquid chromatographic system with fluorometric detection (Shimadzu, Japan).

Surface modification of CrO_2 nanoparticles was carried out, using an ultrasonic homogenizer Sonoplus HD2070 (Bandelin, Germany) and Unimax 1010 orbital shaker (Heidolph, Germany). Centrifugation was carried out with LV-1006 centrifuge (ELMI, Latvia).

The phase composition of obtained MNPs was studied, using a D2 Phaser diffractometer (Bruker, USA), operated at 30 kV, 10 mA, with Cu Kα radiation (wavelength 1.5406 Å). The X-ray diffraction (XRD) pattern was recorded in the 2θ range from 25° to 95° with scanning step of 0.02°. The crystallite size was calculated using Debye-Scherrer's formula for different X-ray reflections.

FTIR spectra were recorded by an IRAffinity-1 spectrophotometer (Shimadzu, Germany) in the region of 400–4000 cm^{-1} using KBr pellets (in case of nanoparticles) or directly in the region of 1500–4000 cm^{-1}, using attenuated total reflection attachment (in case of DES precursors and DES phase).

Morphological analysis was carried out by high-resolution TEM (HRTEM) analysis, using a TM-1000 transmission electron microscope (Hitachi, Japan). The average particle size and their distribution were determined from TEM images within ImageJ program, measuring more than 100 particles. The data were fitted to the log-normal distribution. The mean value of the fit was taken as the average particle size. SEM analysis was performed, using a Zeiss Merlin electron microscope (Carl Zeiss AG, Germany), equipped with EDS detector (Oxford Instruments INCA x-act, Great Britain).

Specific surface area (SSA) was estimated by the Brunauer-Emmett-Teller method on a surface area analyser, Micromeritics ASAP-2020MP (Micromeritics Instrument. Corp., USA). SSA values were calculated based on the TEM data by the following equation: $SSA = \frac{4}{d \cdot \rho}$, where d – nanoparticle thickness, ρ – CrO_2 density. The comparison of experimental and calculated SSA values was used to confirm the accuracy of size estimation from TEM data.

Dynamic light scattering (DLS) experiments and zeta potential analysis were carried out with a SZ100 Analyzer (Horiba Jobin Yvon, Japan).

Magnetic measurements were carried out with a Lake Shore 7410 vibration sample magnetometer (VSM) (Lake Shore Cryotronics, USA) at room temperature.

NMR spectroscopy for DES and its precursors was carried out with a NMR spectrometer Bruker AVANCE IIITM 400 MHz (Bruker, USA).

2.3. Preparation of DESs

DESs were prepared according to procedure presented in literature [36]. The hydrogen bond acceptor (thymol) was mixed with the appropriate fatty acid (hexanoic, heptanoic, octanoic and nonanoic acids) at molar ratio of 1:1, and the mixtures were heated at 60 °C with stirring until transparent viscous liquids were obtained. DESs were stored at room temperature.

2.4. Synthesis of MNPs

The synthesis of CrO_2 nanoparticles was carried out as described in literature [35]. For this, 214.0 g of CrO_3, 82.0 g of Cr_2O_3, 3.3 g of SbC_2O_4OH and 16.5 g of Fe_2O_3 were mixed with 100 mL of ultra-pure water and maintained under hydrothermal conditions at 330°C for 2 h in an autoclave. After that, the autoclave was cooled to room temperature. The resulting black precipitate was collected, washed with ultra-pure water three times for 20 min, and air-dried at 100 °C for 5 h.

For surface modification of MNPs, 200.0 mg of obtained CrO_2 powder, 20.0 mg of carboxylic acid (hexanoic, heptanoic, octanoic or

nonanoic acid) and 5 mL of ultra-pure water were mixed, sonicated (325 W, 35 kHz) for 10 min and shaken for 30 min (1200 rpm). The modified MNPs were collected by centrifugation (7000×*g*, 2 min), washed once with ethanol and freeze-dried.

2.5. Samples

Two different environmental water samples were analyzed. River water (the Neva River, St. Petersburg) and lake water **(**St. Petersburg**)** were collected during the autumn season in glass bottles. Samples were filtered through a hydrophilic (cellulose acetate) filter (0.45 μm) and stored in a dark place at 5 °C. The pH of all samples was in the range of 5–7; thus, no pH adjustment was required.

2.6. Microextraction procedure

10 μL of DES based on thymol and nonanoic acid (molar ratio 1:1) and 5 mL of environmental water sample with pH from 5 to 7 (prepared according to *2.5*) were manually mixed in a polypropylene vial for 3 min (Fig. 1). The collector (chromium dioxide MNPs, modified with nonanoic acid, 5.0 mg) was added to the mixture in the vial, and the resulting suspension was shaken manually for 1 min A magnet was brought to the wall of the vial, and the aqueous phase was aspirated into a syringe, while the collector, dampened by the extract phase, containing analytes, was held by the external magnet. Finally, 50 μL of methanol was added into the vial, and extract dissolution was carried out for 3 min by manual stirring. The MNPs were collected by the magnet, and analyte solution in methanol (30 μL) was aspirated into a chromatographic syringe and introduced into the HPLC-FLD system for analysis.

2.7. HPLC-FLD analysis

Chromatographic separation was carried out with a Supelco C18 column (250 mm × 4.6 mm, 5 μm). Mobile phase, consisting of solvent A (phosphate buffer solution, pH 6.4) and solvent B (methanol), was used for the determination of fluoroquinolones. Separation of analytes was carried out in isocratic elution mode. The concentration of solvent A was 55%, whereas the concentration of solvent B was 45%. The flow-rate was 0.70 mL min^{-1}. The excitation and emission wavelengths were 278 and 456 nm, respectively. The temperature of the chromatographic column was 30 °C. The injection loop volume was 20 μL.

3. Results and discussion

3.1. Optimization of extraction in DES phase

3.1.1. DES composition and preliminary studies

Previously, hydrophobic DESs based on thymol and fatty acids (hexanoic, heptanoic, octanoic, and nonanoic acids) were investigated for fluoroquinolones extraction. In all cases, DESs based on thymol and fatty acids at 1:1 M ratio of precursors were viscous liquids at room temperature. For fluoroquinolones extraction, 100 μL of DES and 2.0 mL of working analyte solution (0.1 mg L-1) were manually mixed for 10 min, and after phase separation by centrifugation (7000×*g*, 3 min), analysis of the aqueous phase and DES phase was performed. The results show that, increase in hydrophobicity of the fatty acid precursor of DES had a positive effect on the extraction recovery (ER, %) (Fig. 2 A). The highest ER was observed for the hydrophobic DES based on thymol and fatty acid with the longest hydrocarbon chain (nonanoic acid) due to its least solubility in aqueous phase.

The effect of molar ratio of DES precursors on the extraction efficiency of fluoroquinolones was also investigated by manual mixing of 500 μL of DES and 500 μL of working analyte solution (0.1 mg L-1) for 10 min, phase separation by centrifugation and further analysis of the aqueous phase and DES phase. Mass transfer of fluoroquinolones in nonanoic acid phase and thymol phase was characterized by 28–40% and 50–80% ER values, respectively. However, DES based on thymol and nonanoic acid with molar ratio of 1:1 showed the best extraction ability (Fig. 2 B); a phenomenon that can be due to synergetic combination of van der Waals forces between aromatic cycles of thymol and fluoroquinolones (π-π interactions) and hydrogen bonding between the hydroxyl group of thymol or carboxyl group of nonanoic acid and the hydroxyl groups of fluoroquinolones (ESM Fig. 1).

The synergetic effect of DES based on thymol and nonanoic acid was confirmed by comparing the experimental and calculated distribution coefficients of extraction. The experimental distribution coefficients were observed to be higher than the coefficients calculated by the additive scheme. The experimental distribution coefficients (D_i) of the extraction system (aqueous phase and DES, 1:1, v/v) were determined as the concentration of fluoroquinolones in DES phase (C_{DES}) divided by their concentration in aqueous phase (C_{aq}) after phase separation: $D_i = C_{DES}/C_{aq}$. The additive distribution coefficients (D_{add}) were calculated for various molar ratios of thymol (χ_1) and nonanoic acid ($\chi 2$): $D_{add} = D_{exp1}\cdot\chi_1 + D_{exp2}\cdot\chi_2$, where D_{exp1} – distribution coefficient for thymol; D_{exp2} – distribution coefficient for nonanoic acid. The synergy coefficient (k) was calculated according to the following equation: $k = lg(\frac{D_{exp}}{D_{add}})$. The dependence of the experimental distribution coefficients on DES composition (extraction isotherms) is represented in Fig. 3. The extraction isotherms, as well as the synergy coefficient values higher than zero (Table 1), indicate the presence of synergetic effect. The optimal DES composition, $\chi_1 = 0.50$ and $\chi_2 = 0.50$, provided the maximum synergetic effect. Among the studied fluoroquinolones, ofloxacin, which is the most hydrophobic analyte, had the highest distribution coefficient.

To confirm the established patterns thermodynamic partition coefficients were determined in the work. Two-phase system consisting of 1-octanol and water is widely used to estimate hydrophilicity of a sub-

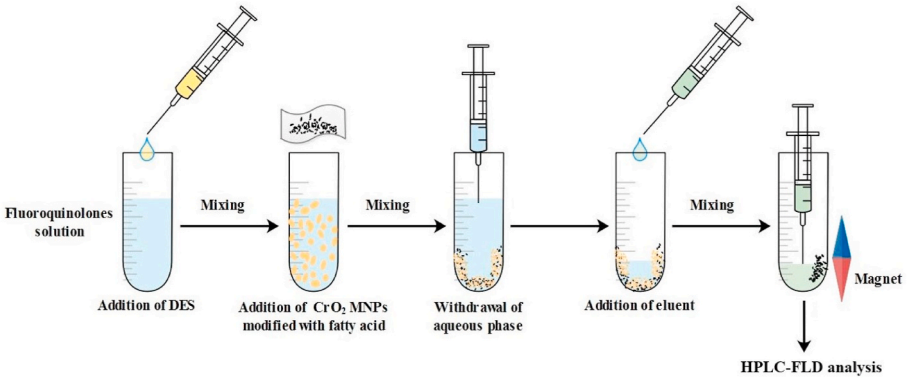

Fig. 1. Graphical representation of LLME with hydrophobic DES followed by magnetic phase separation.

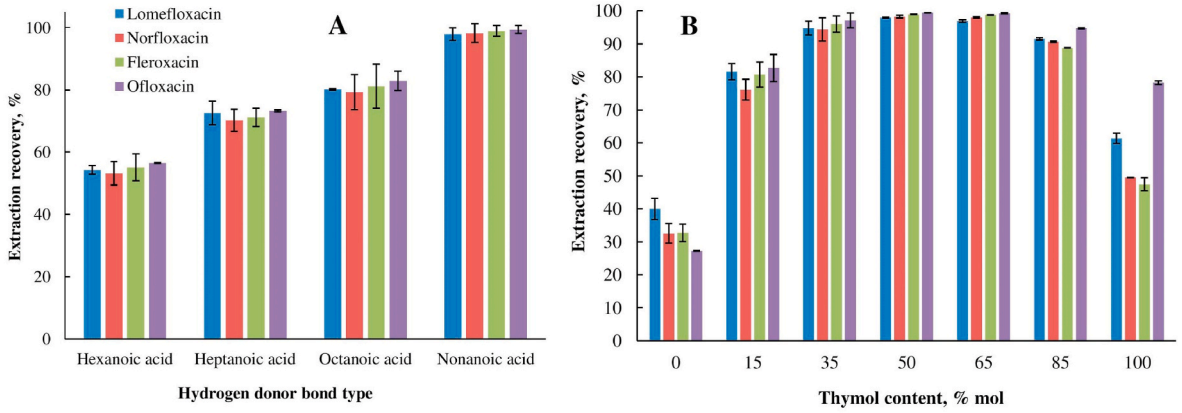

Fig. 2. Investigation of appropriate DES composition for extraction of fluoroquinolones into DES phase (fluoroquinolone concentration 0.1 mg L^{-1}): **A.** Effect of hydrogen bond donor type on extraction recovery (molar ratio of thymol to fatty acid 1:1, volume of sample solution 2.0 mL, volume of DES 100 μL, pH = 6, extraction time 10 min); **B.** Effect of thymol content in DES on extraction recovery (volume of sample solution 500 μL, volume of DES 500 μL, pH = 6, extraction time 10 min).

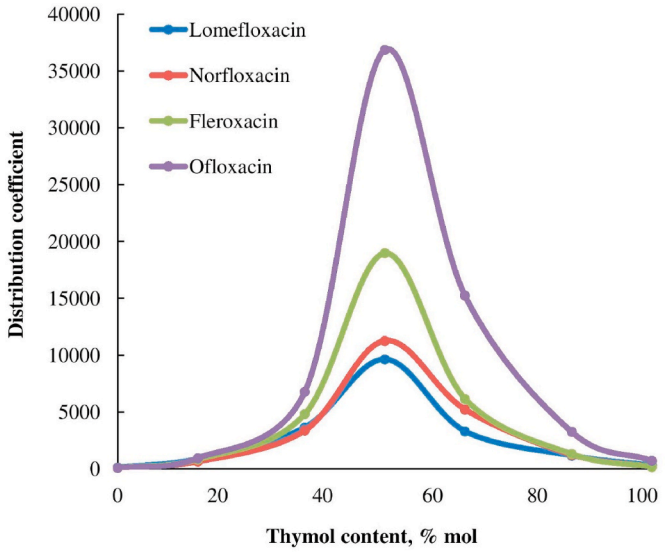

Fig. 3. Effect of DES composition on distribution coefficient (fluoroquinolone concentration 0.1 mg L^{-1}, volume of sample solution 500 μL, volume of DES 500 μL, pH = 6, extraction time 10 min).

stance. Thermodynamic partition coefficients between 1-octanol and water (K_D) is defined as $\frac{\alpha_o}{\alpha_w}$, where α_o is the equilibrium activity of the neutral (zwitterionic and molecular) species in 1-octanol phase, and α_w is the equilibrium activity of the neutral (zwitterionic and molecular) species in aqueous phase. K_D values at pH 7 for norfloxacin, lomefloxacin, fleroxacin and ofloxacin are equal to 0.100, 0.146, 0.294 and 0.526, respectively [37]. A higher K_D value represents a higher hydrophobicity of the analyte, and thus, a greater fraction of the molecules of the analyte are extracted into 1-octanol phase. Thus, K_D values explain distribution coefficients of the analytes in the studied extraction systems; and can be said to have influence on the extraction of analytes in DES phase. Another important feature of these compounds is related to the proportion of their zwitterionic and molecular forms in solution. As can be found in literature [38], the ratios of concentration of zwitterionic form to molecular form for lomefloxacin, fleroxacin, ofloxacin and norfloxacin are 3018, 435, 146 and 118, respectively. This data shows that lomefloxacin has significantly more zwitterionic species compared to the other fluoroquinolones. Norfloxacin, with the lowest K_D value of 0.100, and thus, the least hydrophobic analyte, is mostly in its molecular than zwitterionic form. The oppositely charged groups of zwitterionic species accounts for their higher polarity compared to molecular species.

3.1.2. *Effect of pH*

The pH of aqueous phase has significant influence on the behavior of fluoroquinolones. The analytes studied have two dissociation constants [39]: $pKa_1 = 6.05$ and $pKa_2 = 8.22$ for ofloxacin, $pKa_1 = 5.82$ and $pKa_2 = 9.30$ for lomefloxacin, $pKa_1 = 6.30$ and $pKa_2 = 8.38$ for norfloxacin, and $pKa_1 = 5.46$ and $pKa_2 = 8.10$ for fleroxacin. At pH < pKa_1, analytes exist mainly in cationic forms. Neutral molecular and zwitterionic forms are predominant at pKa_1<pH < pKa_2. At pH > pKa_2, deprotonation of more than 50% of fluoroquinolone molecules occurs with the formation of anionic forms. Since DES based on thymol and nonanoic acid is hydrophobic, mass transfer of neutral molecular and zwitterionic forms to the DES phase can be performed effectively. The effect of pH (1–7) on mass transfer of fluoroquinolones to DES phase was studied. The pH of each working solution was adjusted with 1 mol L^{-1} HCl or NaOH. Then, 100 μL of DES was added to 4 mL of the solution, and manually mixed for 10 min. Phase separation was carried out by centrifugation before phases analysis. Mass transfer in alkaline media was not studied because the DES decomposes in such conditions due to the ionization of thymol and nonanoic acid. It was found that pH less than 5 resulted in decreasing ERs because fluoroquinolones exist in cationic forms at these conditions (Fig. 4 A). Therefore, neutral media is more appropriate for fluoroquinolones mass transfer.

3.1.3. *Effect of DES volume*

The extraction solvent volume is an important microextraction parameter, which can influence the ER, EF, as well as the sensitivity of the developed method. Varied volumes (5–80 μL) of DES were injected into 5 mL of aqueous sample with a micropipette. Manual mixing was carried out for 10 min, followed by centrifugation and aqueous phase aspiration for further analysis. High viscosity of DES phase makes its collection in micro-liter amounts (less 50 μL) difficult and irreproducible. The reproducibility of analyte extraction in DES phase is an important factor for providing suitable overall reproducibility of the microextraction procedure. To estimate effect of the extraction solvent volume in micro-liter amounts only aqueous phase was analyzed after centrifugation. The initial and residual concentrations of fluoroquinolones in the aqueous phase were considered to calculate EFs. High EFs and satisfactory reproducibility values were achieved, using 10.0 μL of DES (Fig. 4 B). Higher DES volumes led to dilution effect.

3.1.4. *Effect of ionic strength*

It is known that the ionic strength of a sample solution can affect ERs

Table 1
Distribution coefficients and synergy coefficients for DESs based on thymol and nonanoic acid.

Molar ratios of thymol	D_{exp}				D_{add}				k			
	Lomefloxacin	Norfloxacin	Fleroxacin	Ofloxacin	Lomefloxacin	Norfloxacin	Fleroxacin	Ofloxacin	Lomefloxacin	Norfloxacin	Fleroxacin	Ofloxacin
0	133	97	97	75	133	97	97	75	0	0	0	0
0.15	885	639	835	954	161	112	110	172	0.7	0.8	0.9	0.7
0.35	3641	3366	4812	6769	198	131	126	301	1.3	1.4	1.6	1.4
0.50	9646	11,278	18,981	36,860	225	146	139	397	1.6	1.9	2.1	2.0
0.65	3321	5236	6175	15,253	253	161	151	494	1.4	1.8	2.0	1.8
0.85	1177	1251	1309	3253	290	181	168	623	0.9	1.0	1.0	0.8
1.00	318	196	180	720	318	196	180	720	0	0	0	0

[40]. Different widely-used salting-out agents (sodium chloride, sodium sulfate, and sodium nitrate) were studied at 5% concentration in the sample. The experimental investigations showed no difference in ER values with or without the salting-out agents (ESM Fig. 2 A). Thus, further studies were performed without addition of salts.

3.1.5. Effect of extraction time

To study the effect of extraction time on mass transfer of fluoroquinolones, 10.0 μL of DES was chosen for analyte separation. In this instance, slow extraction kinetics could be observed due to high sample-to-extractant phase ratio. The aspirated aqueous phases after extraction were analyzed as mentioned before. Mixing time of 3 min was optimum to obtain equilibrium in the extraction system (ESM Fig. 2 B).

3.2. Optimization of DES phase collection with MNPs

Though, 10.0 μL of the extract could not be reproducibly aspirated with pipette, MNPs served as an effective extract phase collector. In this research, MNPs based on surface modification of CrO_2 particles with 6–9 hydrocarbon chain fatty acids were investigated as collectors of the extract phase. CrO_2 was chosen based on its stability and excellent magnetic properties [35]. The data on characterization of obtained MNPs is presented in Section 3.4.2.

The highest chromatographic peak areas were observed for MNPs with surface modified by octanoic and nonanoic acids (ESM Fig. 3 A). These two types of MNPs, with sparse modification layer, exhibit stronger magnetic characteristics according to the data presented in Section 3.4.2. Sparsity of the modified surface layer of MNPs promotes both hydrophilic and hydrophobic interactions between MNPs and DES containing analytes. This phenomenon is in agreement with reported observation in literature [41]. Stronger hydrophobic interactions were observed between DES and the MNPs with increasing length of hydrocarbon chain of fatty acids as surface-modifiers. Further experiments were conducted with CrO_2 MNPs, modified with nonanoic acid, due to low solubility of the modifier; and thus, high stability of the MNPs in aqueous phase.

The available collector surface area depends on the mass of nanoparticles. The mass of nanoparticles was varied in the range of 1–7 mg; and 5.0 mg was chosen as optimal, because this provided maximum chromatographic peak areas at minimum nanoparticles consumption (ESM Fig. 3 B).

3.3. Elution procedure optimization

Elution of DES phase containing analyte from the collector was required to obtain solution compatible with HPLC-FLD system. The elution efficiency depends on the properties of the eluent. Three polar solvents (acetonitrile, methanol, and isopropanol) were investigated as eluents; and satisfactory separation of the analyte signals under the selected chromatographic conditions was achieved only with methanol. Thus, for the best compatibility with chromatographic separation, methanol was used as a component of the mobile phase.

The effect of eluent volume on chromatographic peak areas was studied. Minimum eluent volume of 50 μL provided maximum peak area values (ESM Fig. 4 A). At higher eluent volume, dilution effect was observed.

Different elution times (1, 3 and 5 min) were also studied. It was established that mass transfer in methanol was fast, and 3 min was enough to complete the elution of fluoroquinolones from the collector (ESM Fig. 4 B). The chromatograms of the initial aqueous solution of fluoroquinolones and eluate from MNPs are presented in ESM Fig. 5.

3.4. Investigation of extraction phase and extract collector

3.4.1. Characterization of DES

To confirm the formation of DES, ^{1}H NMR and FTIR spectra of

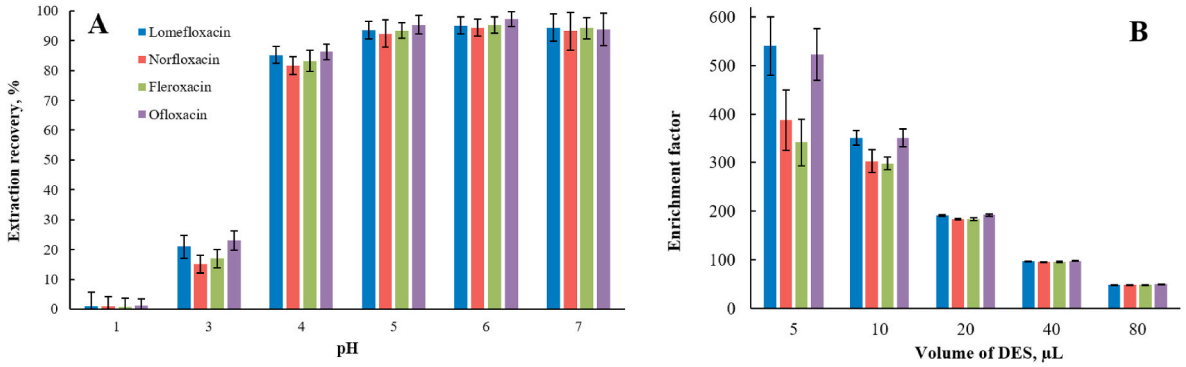

Fig. 4. Investigation of appropriate experimental conditions for extraction of fluoroquinolones into DES phase (fluoroquinolone concentration 0.1 mg L^{-1}): **A.** Effect of pH on extraction recovery (molar ratio of thymol to nonanoic acid 1:1, volume of sample solution 5 mL, volume of DES 10 µL, extraction time 10 min); **B.** Effect of volume of DES on extraction recovery (molar ratio of thymol to nonanoic acid 1:1, volume of sample solution 5 mL, pH = 6, extraction time 10 min).

thymol, nonanoic acid and DES were obtained (ESM Figs. 6 and 7). ^{1}H NMR spectra were recorded in $CDCl_3$ and calibrated according to the residual peak of $CHCl_3$ (7.26 ppm). In the DES spectrum, the signals corresponding to the proton of the hydroxyl group of thymol at 4.62 ppm and the proton of the carboxyl group of nonanoic acid at 11.10 ppm were shifted, overlapped and formed one broad peak at 7.65 ppm. Thus, displacement of signals related to the protons of the carboxyl group of nonanoic acid, and the hydroxyl group of thymol was observed. The formation of hydrogen bond led to the proton belonging simultaneously to two molecules (thymol and nonanoic acid). Furthermore, signal broadening was observed because of the formation of hydrogen bonds and active intermolecular proton exchange between the two precursors; and thus, the ^{1}H NMR spectrometer recorded all the positions of the bound proton in time. This phenomenon can be considered as a confirmation of the formation of DES [42]. Additional confirmation is the shift of peak corresponding to the stretching vibration of the hydroxyl group of thymol from 3250 to 3420 cm^{-1} in the FTIR spectrum along with its broadening, showing the involvement of the hydroxyl group in hydrogen bond formation, as reported in literature [43,44].

3.4.2. *Characterization of MNPs*

In accordance with XRD data (ESM Fig. 8 A), as-prepared CrO_2 MNPs have a common tetragonal $P4_2/mnm$ crystal structure (marked as filled square, ICDD card # 01-084-1821). The observed two low intensity peaks from Cr_2O_3 (marked with open circles, ICDD card # 01-070-3766, 6% based on semi-quantitative analysis) correspond to the transfer from bulk CrO_2 phase and surface β-CrOOH phase (marked as open squares, ICDD card # 01-070-1115).

TEM image (ESM Fig. 8 B) demonstrated the needle-like nanoparticles with the thickness of 20.5 ± 1.0 nm (ESM Fig. 8 B, in the insert). The obtained result was in good agreement with SEM data (ESM Fig. 9 A) and experimental SSA value of 30 m^2 g^{-1}. In addition, the MNPs crystallite size, calculated from XRD data, was equal to 23.9 ± 1.0 nm. The close value of TEM size and XRD crystallite size indicated that MNPs are monocrystalline. This was confirmed by SAED data (selected area of electron diffraction, ESM Fig. 8 D), which shows the single points that are typical for monocrystalline samples.

The FTIR spectra of CrO_2 MNPs (ESM Fig. 10, grey line) shows the peaks related to CrO_2 in a range of 500–1200 cm^{-1}, marked as filled square [45,46]. The additional peaks detected near 470, 1400 and 1520 cm^{-1}, marked as open square, are associated with β-CrOOH [45,46]. Furthermore, the peaks observed at 1618 and 3430 cm^{-1} are typical for oxide materials and are caused by surface hydroxyl groups and adsorbed water.

The VSM data for CrO_2 MNPs (ESM Fig. 8 C) represent the typical ferromagnetic behavior with the expressed magnetic saturation and coercivity value equal to 625 Oe (ESM Table 1). In accordance with XRD data (ESM Fig. 8 A, open squares, 9% based on semi-quantitative analysis), FTIR data (ESM Fig. 10, grey line) and TEM data (ESM Fig. 8 E, highlighted with red rectangle), the obtained nanoparticles show the presence of β-CrOOH surface layer. This was formed due to careful and prolonged washing of the MNPs; which can provide simple and fast surface modification for the MNPs with fatty acids via the interaction between nanoparticle surface hydroxyl groups and fatty acid carboxyl groups. Hexanoic, heptanoic, octanoic and nonanoic acids were used as surface-modifiers to ensure hydrophobicity of the nanoparticles.

The successful modification was confirmed by FTIR spectroscopy data (ESM Fig. 10). In addition to the peaks related to CrO_2 (marked as filled square), β-CrOOH (marked as open square) [45,46], surface hydroxyl groups and adsorbed water (marked as filled circle), the peaks observed in the region of 2800–3000 cm^{-1} (marked with a dot rectangle) are related to CH_2 symmetric and asymmetric vibrations of hydrocarbon chains of fatty acids. These peaks are well-distinguished and are of expressed intensity, indicating the successful surface modification of the MNPs. In addition, the peaks observed near 1630 and 3440 cm^{-1} show abrupt changes in intensity for the MNPs modified with hexanoic and nonanoic acids in comparison with the unmodified MNPs. The low intensity peaks near 2300 cm^{-1} (related to sorbed CO_2 molecules) also became more expressed. This points to a particular arrangement of the modifiers on the MNPs surface, leading to more expressed sorption of gaseous molecules from air.

According to the SEM data, all the MNPs have needle-like, agglomerated structure, and are very similar to each other, which indicates that the surface modification, as expected, did not affect MNPs size and shape. EDX analysis (see data in the Table in ESM Fig. 9) shows that the amount of carbon is zero for unmodified MNPs and increases from 2.9 at % up to 12.5 at% with increase in hydrocarbon chain of fatty acid. This confirms that an equal number of fatty acid molecules (independent of their hydrocarbon chain) are attached to the same MNPs surface area during modification.

The data presented in ESM Fig. 11 and summarized in ESM Table 1 demonstrates a typical ferromagnetic behavior of MNPs with high values of saturation magnetization, which is required for simple and fast collection of MNPs with a magnet.

The remanence (M_R) to saturation magnetization (M_S) ratio (i.e. M_R: M_S) is not strongly influenced by the surface modification. At the same time, the coercivity, responsible for the stability of the MNP agglomerates (formed under the influence of magnetic field) during the extraction procedure, depends on the fatty acid chain length, and attained maximal value for the CrO_2 MNPs modified with nonanoic acid. This phenomenon can be explained by the physical interaction between single-domain MNPs via the hydrophobic tail of the modifying fatty acid, followed by particle-particle magnetic interactions. It is important to note that the formed agglomerates (more expressed in the case of nonanoic acid than the other fatty acids) can be destroyed by physical impact on the system

in the elution step, resulting in well-distinguishable disaggregated MNPs.

As can be seen from ESM Table 1, surface modification led to decrease in zeta (ζ)-potential values, which can be used for estimation of the surface charge of MNPs in aqueous solution. Contrary to hexanoic and heptanoic acids forming a dense layer on the surface of MNPs, resulting in sharp decrease of surface charge, octanoic and nonanoic acids with longer hydrocarbon chains formed a sparse layer, with slight changes in the surface charge. These results are supported by hydrodynamic size measurements. Surface modification with octanoic and nonanoic acids resulted in minimal sizes of MNP agglomerates, which usually appear when nanoparticles are placed in a liquid phase. It should be pointed out, that the trend for zeta-potential change is similar to the variation of oxygen percent by EDX, which can be explained by the special arrangement of fatty acid molecules on MNPs surface.

3.5. Analytical performance

Feasibility of the developed procedure was evaluated based on relevant parameters such as linear range, determination coefficient, limit of detection (LOD), limit of quantification (LOQ) and precision (Table 2).

For each fluoroquinolone, the calibration curve was obtained by plotting peak area *vs* concentration (n = 3). The values of LOD calculated from a blank test based on 3σ (standard deviation of the peak area values for blank sample) were 0.01 μg L^{-1} for ofloxacin, 0.02 μg L^{-1} for lomefloxacin and fleroxacin, and 0.04 μg L^{-1} for norfloxacin. For peak area values equal to 10σ, the LOQ was 0.03 μg L^{-1} for ofloxacin, 0.06 μg L^{-1} for lomefloxacin and fleroxacin, and 0.12 μg L^{-1} for norfloxacin.

The intra-day and inter-day precision was expressed as relative standard deviation (RSD) of analyte content that ranged from 3 to 5% and from 7 to 10%, respectively. ERs and EFs were in the range of 90–99% and 90 to 99, respectively.

To assess greenness of the developed approach, the analytical eco-scale assessment tool proved to be a good, semiquantitative procedure for this purpose [47,48]. Ideal green procedure has a total score of 100 with no penalty points. Penalty points depend on the harmful impacts of the approach on the environment (i.e. toxicity of the chemicals, energy consumption, the amount of waste generated), which are subtracted from the total score. The penalty points for the determination of fluoroquinolones by the proposed technique are summarized in ESM Table 2. The total score was 85, demonstrating that the approach is green (>75 of the total score according to the assessment tool).

Table 2
Analytical characteristics of the developed procedure.

Parameters	Analyte			
	Lomefloxacin	Norfloxacin	Fleroxacin	Ofloxacin
Linear range, μg L^{-1}	0.06–15.0	0.12–15.0	0.06–15	0.03–15.0
Intercept	4281	15,851	10,423	48,927
Slope	30,597	60,301	11,125	91,696
Determination coefficient, r^2	0.996	0.998	0.997	0.996
Limit of detection, μg L^{-1}	0.02	0.04	0.02	0.01
Limit of quantification, μg L^{-1}	0.06	0.12	0.06	0.03
Relative standard deviation (n = 3), % Intra-day (C = 0.12 or 15.0 μg L^{-1})	3	4	4	5
Inter-day (C = 0.12 or 15.0 μg L^{-1})	7	9	8	10
Extraction recovery, %	95	94	95	97
Enrichment factor	95	94	95	97

3.6. Analysis of real samples

The proposed procedure was applied to the analysis of river and lake water samples. Fluoroquinolones were not found in all the environmental water samples (Table 3). To study the accuracy of the procedure, two different samples were spiked at various concentration levels in order to calculate the relative recoveries for each analyte. The spiked concentration levels were chosen based on usually found residue levels of fluoroquinolones in environmental waters (up to 10 μg L^{-1}) [49]. As can be seen in Table 3, good relative recoveries were obtained (from 89 to 101%), proving that there is no interfering effect of sample matrix. Additionally, no interfering peaks were observed during chromatographic analysis of real samples (ESM Fig. 12).

3.7. Comparison of the developed procedure with other procedures

The main figure of merits values for proposed and reported sample preparation procedures using DES for fluoroquinolone determination in different matrices by various analytical techniques are indicated in Table 4. As can be seen, other liquid-liquid microextraction approaches require relatively high volume of the extraction solvent to be used and more than 20 min for sample preparation. In case of solid-phase extraction, additional sample preparation steps and analytical equipment are required. Unlike these reported microextraction procedures for fluoroquinolone determination, the developed procedure requires minimum DES volume consumption (down to 10 μL), and provides less LODs and higher throughput along with comparable sample amount.

4. Conclusion

In this work, specially produced MNPs based on chromium dioxide with a fatty acid surface layer were successfully applied to hydrophobic DES phase (extract) collection after LLME. The developed approach allowed to significantly reduce the extraction solvent (DES) volume (down to 10 μL). To analyze the extract by the HPLC-FLD method, it was eluted from the collector by a polar solvent. The obtained extract solution in the polar solvent was compatible with water-polar organic solvent mobile phase, because it contains minimum amount of hydrophobic DES precursors. The developed sample preparation procedure was used for the sensitive determination of fluoroquinolones in environmental waters by HPLC-FLD. Time of sample pretreatment was less than 8 min, using 10 μL of DES, 5 mg of MNPs and 50 μL of methanol. This is significant for reaching the main goals of sustainable growth and development, such as minimizing resource consumption, toxic material use, waste and pollutants generated throughout the entire chemical analysis process. According to the analytical eco-scale assessment tool, the proposed approach is green and environmentally friendly. The obtained LODs allowed to determine fluoroquinolones at levels less than usually found in environmental waters.

Credit author statement

Aleksei Pochivalov: Conceptualization, Methodology, Writing – original draft, Investigation. Kseniia Cherkashina: Supervision, Formal analysis, Visualization, Investigation. Andrey Sudarkin: Formal analysis, Visualization, Investigation, Data curation. Mikhail Osmolowsky: Conceptualization, Methodology. Olga Osmolovskaya: Conceptualization, Formal analysis, Visualization, Investigation, Data curation. Firuza Krekhova: Formal analysis, Visualization, Investigation, Data curation. Lawrence Nugbienyo: Data curation, Writing – review & editing. Andrey Bulatov: Conceptualization, Supervision, Writing – review & editing.

Declaration of competing interest

The authors declare that they have no known competing financial interests or personal relationships that could have appeared to influence

Table 3
Determination of fluoroquinolones in water samples (n = 3, P = 0.95).

Sample	Added, μg L^{-1}				Found, μg L^{-1}				Relative recovery, %			
	FLERO	LOME	NOR	OFLX	FLERO	LOME	NOR	OFLX	FLERO	LOME	NOR	OFLX
River water	0	0	0	0	<LOD	<LOD	<LOD	<LOD	–	–	–	–
	0.25	0.25	0.25	0.25	0.25 ± 0.02	0.24 ± 0.05	0.24 ± 0.04	2.4 ± 0.4	100	96	96	96
	5.0	5.0	5.0	5.0	4.6 ± 0.6	4.8 ± 0.5	5.1 ± 0.5	4.9 ± 0.6	92	96	102	98
	10.0	10.0	10.0	10.0	9.7 ± 0.5	9.3 ± 0.6	9.3 ± 0.4	9.9 ± 0.7	97	93	93	99
Lake water	0	0	0	0	<LOD	<LOD	<LOD	<LOD	–	–	–	–
	0.25	0.25	0.25	0.25	0.22 ± 0.03	0.22 ± 0.06	0.24 ± 0.05	0.23 ± 0.06	88	88	96	92
	5.0	5.0	5.0	5.0	4.5 ± 0.6	4.6 ± 0.5	4.9 ± 0.5	4.8 ± 0.6	90	92	98	96
	10.0	10.0	10.0	10.0	9.7 ± 0.7	9.5 ± 0.5	9.0 ± 0.5	9.9 ± 0.4	97	95	90	99

FLERO – fleroxacin, LOME – lomefloxacin, NOR – norfloxacin, OFLX – ofloxacin.

Table 4
Figure of merits for proposed and reported sample preparation procedures using DES for the fluoroquinolones determination.

Method	Sample	Sample preparation	DES	Sample amount	Extractant volume, μL	Extraction time, min	LOD	RSD, %	Relative recovery, %	Ref.
qNMR	Pharma-ceuticals	DLLME	methyltrioctyl-ammonium bromide and decanoic acid	15 g	200	20	100 μg L^{-1} for gatifloxacin, levofloxacin, enrofloxacin, ciprofloxacin, sparfloxacin	6	>92	[50]
MECC	Water	DLLME	methyltrioctyl ammonium bromide and decanoic acid	5 g	200	20	6 μg L^{-1} for sparfloxacin, enrofloxacin; 10 μg L^{-1} for gatifloxacin, ciprofloxacin, lomefloxacin, levofloxacin	7.6	88–114	[51]
HPLC-FLD	Meat	LLME	tetrabutylam-monium bromide and 1-heptanol	0.2 g	–	30	10 μg kg^{-1} for ofloxacin, 15 μg kg^{-1} for fleroxacin	4–10	98–100	[52]
HPLC-UV	Milk	SPE	choline chloride and glycerol	20 mL	–	–	500 μg L^{-1} for levofloxacin	<5.4	88.3–101.5	[53]
HPLC-FLD	Environ-mental water	LLME	thymol and nonanoic acid	5 mL	10	8	0.01 μg L^{-1} for ofloxacin, 0.02 μg L^{-1} for lomefloxacin and fleroxacin, and 0.04 μg L^{-1} for norfloxacin	<14	89–101	This work

qNMR – quantitative nuclear magnetic resonance; DLLME – dispersive liquid-liquid microextraction; MECC – micellar electrokinetic capillary chromatography; LLME – liquid-liquid microextraction; HPLC-UV – high performance liquid chromatography with spectrophotometric detection in the ultraviolet region of the spectrum; SPE – solid phase extraction; HPLC-FLD – high performance liquid chromatography with fluorometric detection.

the work reported in this paper.

Data availability

The authors are unable or have chosen not to specify which data has been used.

Acknowledgements

The authors gratefully acknowledge the Russian Science Foundation (project no. № 21-13-00020, https://rscf.ru/project/21-13-00020/). Scientific research was performed using the equipment of the Research Park of St. Petersburg State University (Chemical Analysis and Materials Research Centre, Centre for Magnetic Resonance, Centre of Thermal Analysis and Calorimetry, Centre for X-ray Diffraction Studies, Centre for Innovative Technologies of Composite Nanomaterials, Centre for Optical and Laser Materials Research, Interdisciplinary Resource Centre for Nanotechnology).

Appendix A. Supplementary data

Supplementary data to this article can be found online at https://doi.org/10.1016/j.talanta.2022.123868.

References

[1] Y.P. Mbous, M. Hayyan, A. Hayyan, W.F. Wong, M.A. Hashim, C.Y. Looi, Applications of deep eutectic solvents in biotechnology and bioengineering—promises and challenges, Biotechnol. Adv. 35 (2017) 105–134, https://doi.org/10.1016/j.biotechadv.2016.11.006.

[2] A. Hayyan, F.S. Mjalli, I.M. Alnashef, Y.M. Al-Wahaibi, T. Al-Wahaibi, M. A. Hashim, Glucose-based deep eutectic solvents: physical properties, J. Mol. Liq. 178 (2013) 137–141, https://doi.org/10.1016/j.molliq.2012.11.025.

[3] I.M. Aroso, A. Paiva, R.L. Reis, A.R.C. Duarte, Natural deep eutectic solvents from choline chloride and betaine – physicochemical properties, J. Mol. Liq. 241 (2017) 654–661, https://doi.org/10.1016/j.molliq.2017.06.051.

[4] B. Kudłak, K. Owczarek, J. Namieśnik, Selected issues related to the toxicity of ionic liquids and deep eutectic solvents—a review, Environ. Sci. Pollut. Res. 22 (2015) 11975–11992, https://doi.org/10.1007/s11356-015-4794-y.

[5] T. Zhang, T. Doert, H. Wang, S. Zhang, M. Ruck, Inorganic synthesis based on reactions of ionic liquids and deep eutectic solvents, Angew. Chem. Int. Ed. 60 (2021) 22148–22165, https://doi.org/10.1002/anie.202104035.

[6] D.A. Alonso, A. Baeza, R. Chinchilla, G. Guillena, I.M. Pastor, D.J. Ramón, Deep eutectic solvents: the organic reaction medium of the century, Eur. J. Org Chem. 2016 (2016) 612–632, https://doi.org/10.1002/ejoc.201501197.

[7] A.P. Abbott, K. El Ttaib, G. Frisch, K.S. Ryder, D. Weston, The electrodeposition of silver composites using deep eutectic solvents, Phys. Chem. Chem. Phys. 14 (2012) 2443–2449, https://doi.org/10.1039/c2cp23712a.

[8] D. Nguyen, T. Van Huynh, V.S. Nguyen, P.L. Doan Cao, H.T. Nguyen, T.C. Wei, P. H. Tran, P.T. Nguyen, Choline chloride-based deep eutectic solvents as effective electrolytes for dye-sensitized solar cells, RSC Adv. 11 (2021) 21560–21566, https://doi.org/10.1039/d1ra03273a.

[9] W. da Silva, A.C. Queiroz, C.M.A. Brett, Poly(methylene green) – ethaline deep eutectic solvent/Fe2O3 nanoparticle modified electrode electrochemical sensor for the antibiotic dapsone, Sensor. Actuator. B Chem. 325 (2020), 128747, https://doi.org/10.1016/j.snb.2020.128747.

[10] P. Pidenko, C. Vakh, A. Shishov, J. Skibina, N. Burmistrova, A. Bulatov, Microstructured optical fibers sensor modified by deep eutectic solvent: liquid-phase microextraction and detection in one analytical device, Talanta 232 (2021), 122305, https://doi.org/10.1016/j.talanta.2021.122305.

[11] S. Sadeghi, A. Davami, Ternary deep eutectic solvent modified cadmium selenide quantum dots as a selective fluorescent probe for sensing of uranyl ions in water samples, J. Mol. Liq. 316 (2020), 113753, https://doi.org/10.1016/j.molliq.2020.113753.

[12] A. Shishov, A. Bulatov, M. Locatelli, S. Carradori, V. Andruch, Application of deep eutectic solvents in analytical chemistry, A review, Microchem. J. 135 (2017) 33–38, https://doi.org/10.1016/j.microc.2017.07.015.

[13] A. Shishov, A. Gorbunov, L. Moskvin, A. Bulatov, Decomposition of deep eutectic solvents based on choline chloride and phenol in aqueous phase, J. Mol. Liq. 301 (2020), 112380, https://doi.org/10.1016/j.molliq.2019.112380.

[14] C. Florindo, L.C. Branco, I.M. Marrucho, Development of hydrophobic deep eutectic solvents for extraction of pesticides from aqueous environments, Fluid Phase Equil. 448 (2017) 135–142, https://doi.org/10.1016/j.fluid.2017.04.002.

[15] A.R. Zarei, M. Nedaei, S.A. Ghorbanian, Ferrofluid of magnetic clay and menthol based deep eutectic solvent: application in directly suspended droplet microextraction for enrichment of some emerging contaminant explosives in water and soil samples, J. Chromatogr. A 1553 (2018) 32–42, https://doi.org/10.1016/j.chroma.2018.04.023.

[16] Z.G. Shi, H.K. Lee, Dispersive liquid-liquid microextraction coupled with dispersive μ-solid-phase extraction for the fast determination of polycyclic aromatic hydrocarbons in environmental water samples, Anal. Chem. 82 (2010) 1540–1545, https://doi.org/10.1021/ac9023632.

[17] J. Zhang, M. Li, M. Yang, B. Peng, Y. Li, W. Zhou, H. Gao, R. Lu, Magnetic retrieval of ionic liquids: fast dispersive liquid-liquid microextraction for the determination of benzoylurea insecticides in environmental water samples, J. Chromatogr. A 1254 (2012) 23–29, https://doi.org/10.1016/j.chroma.2012.07.051.

[18] D.P. Arcon, F.C. Franco, All-fatty acid hydrophobic deep eutectic solvents towards a simple and efficient microextraction method of toxic industrial dyes, J. Mol. Liq. 318 (2020), 114220, https://doi.org/10.1016/j.molliq.2020.114220.

[19] N. Chaabene, K. Ngo, M. Turmine, V. Vivier, New hydrophobic deep eutectic solvent for electrochemical applications, J. Mol. Liq. 319 (2020), 114198, https://doi.org/10.1016/j.molliq.2020.114198.

[20] A.P. Abbott, G. Capper, D.L. Davies, R.K. Rasheed, V. Tambyrajah, Novel solvent properties of choline chloride/urea mixtures, Chem. Commun. (2003) 70–71, https://doi.org/10.1039/b210714g.

[21] Á. Santana-Mayor, R. Rodríguez-Ramos, A.V. Herrera-Herrera, B. Socas-Rodríguez, M.Á. Rodríguez-Delgado, Deep eutectic solvents. The new generation of green solvents in analytical chemistry, TrAC, Trends Anal. Chem. 134 (2021), 116108, https://doi.org/10.1016/j.trac.2020.116108.

[22] K. Zhang, S. Li, Y. Wang, J. Fan, G. Zhu, Air-assisted liquid-liquid microextraction based on solidification of floating deep eutectic solvent for the analysis of ultraviolet filters in water samples by high performance liquid chromatography with the aid of response surface methodology, J. Chromatogr. A 1618 (2020), 460876, https://doi.org/10.1016/j.chroma.2020.460876.

[23] W. Tang, Y. Dai, K.H. Row, Evaluation of fatty acid/alcohol-based hydrophobic deep eutectic solvents as media for extracting antibiotics from environmental water, Anal. Bioanal. Chem. 410 (2018) 7325–7336, https://doi.org/10.1007/s00216-018-1346-6.

[24] M. Yang, K. Hong, X. Li, F. Ge, Y. Tang, Freezing temperature controlled deep eutectic solvent dispersive liquid-liquid microextraction based on solidification of floating organic droplets for rapid determination of benzoylureas residual in water samples with assistance of metallic salt, RSC Adv. 7 (2017) 56528–56536, https://doi.org/10.1039/c7ra11030h.

[25] K. Cherkashina, A. Pochivalov, F. Shakirova, A. Shishov, A. Bulatov, Microextraction of tetracyclines from milk into deep eutectic solvents for subsequent determination by high performance liquid chromatography-tandem mass spectrometry, J. Anal. Chem. 77 (2022) 255–262, https://doi.org/10.31857/S0044450222030045 ([in Russian]).

[26] M.I. Leong, S. Da Huang, Dispersive liquid-liquid microextraction method based on solidification of floating organic drop combined with gas chromatography with electron-capture or mass spectrometry detection, J. Chromatogr. A 1211 (2008) 8–12, https://doi.org/10.1016/j.chroma.2008.09.111.

[27] K. Zhang, Y. Wang, S. Li, G. Zhu, Air-assisted liquid-liquid microextraction based on the solidification of floating deep eutectic solvents for the simultaneous determination of bisphenols and polycyclic aromatic hydrocarbons in tea infusions via HPLC, Food Chem. 348 (2021), 129106, https://doi.org/10.1016/j.foodchem.2021.129106.

[28] K. Zhang, R. Guo, Y. Wang, Q. Nie, G. Zhu, One-step derivatization and temperature-controlled vortex-assisted liquid-liquid microextraction based on the solidification of floating deep eutectic solvents coupled to UV–Vis spectrophotometry for the rapid determination of total iron in water and food samples, Food Chem. 384 (2022), 132414, https://doi.org/10.1016/j.foodchem.2022.132414.

[29] X. Liu, Y. Bian, J. Zhao, Y. Wang, L. Zhao, Menthol-based deep eutectic solvent in dispersive liquid-liquid microextraction followed by solidification of floating organic droplet for the determination of three bisphenols with UPLC-MS/MS, Microchem. J. 159 (2020), 105438, https://doi.org/10.1016/j.microc.2020.105438.

[30] M.Á. Aguirre, A. Canals, Magnetic deep eutectic solvents in microextraction techniques, TrAC, Trends Anal. Chem. 146 (2022), 116500, https://doi.org/10.1016/j.trac.2021.116500.

[31] M. Karimi, A.M.H. Shabani, S. Dadfarnia, Deep eutectic solvent-mediated extraction for ligand-less preconcentration of lead and cadmium from environmental samples using magnetic nanoparticles, Microchim. Acta 183 (2016) 563–571, https://doi.org/10.1007/s00604-015-1671-9.

[32] M.L. Daly, D.C. Silverstein, Fluoroquinolones, in: Small Anim. Crit. Care Med, second ed., Elsevier Health Sciences, 2014, pp. 934–939, https://doi.org/10.1016/B978-1-4557-0306-7.00178-1.

[33] A. Speltini, M. Sturini, F. Maraschi, A. Profumo, Fluoroquinolone antibiotics in environmental waters: sample preparation and determination, J. Separ. Sci. 33 (2010) 1115–1131, https://doi.org/10.1002/jssc.200900753.

[34] J. Hu, W. Wang, Z. Zhu, H. Chang, F. Pan, B. Lin, Quantitative structure-activity relationship model for prediction of genotoxic potential for quinolone antibacterials, Environ. Sci. Technol. 41 (2007) 4806–4812, https://doi.org/10.1021/es070031v.

[35] D.I. Arkhipov, N.P. Bobrysheva, E.L. Dzidziguri, M.G. Osmolowsky, O. M. Osmolovskaya, Thermal stability of modified chromium dioxide nanopowders with various magnetic properties obtained by hydrothermal route, J. Therm. Anal. Calorim. 128 (2017) 71–78, https://doi.org/10.1007/s10973-016-5919-3.

[36] K. Cherkashina, A. Pochivalov, V. Simonova, F.M. Shakirova, A. Shishov, A. Bulatov, Synergistic effect of hydrophobic deep eutectic solvent based on terpenoids and carboxylic acids for tetracyclines microextraction, Analyst 146 (2021) 3449–3453, https://doi.org/10.1039/D1AN00096A.

[37] D.L. Ross, S.K. Elkinton, C.M. Riley, Physicochemical properties of the fluoroquinolone antimicrobials. III. 1-Octanol/water partition coefficients and their relationships to structure, Int. J. Pharm. 88 (1992) 379–389.

[38] D.L. Ross, C.M. Riley, Physicochemical properties of the fluoroquinolone antimicrobials. II. Acid ionization constants and their relationship to structure, Int. J. Pharm. 83 (1992) 267–272.

[39] D.L. Ross, C.M. Riley, Physicochemical properties of the fluoroquinolone antimicrobials V. Effect of fluoroquinolone structure and pH on the complexation of various fluoroquinolones with magnesium and calcium ions, Int. J. Pharm. 93 (1993) 121–129, https://doi.org/10.1016/0378-5173(93)90170-K.

[40] A.M. Hyde, S.L. Zultanski, J.H. Waldman, Y.L. Zhong, M. Shevlin, F. Peng, General principles and strategies for salting-out informed by the Hofmeister series, Org. Process Res. Dev. 21 (2017) 1355–1370, https://doi.org/10.1021/acs.oprd.7b00197.

[41] K. Cherkashina, M. Voznesenskiy, O. Osmolovskaya, C. Vakh, A. Bulatov, Effect of surfactant coating of Fe_3O_4 nanoparticles on magnetic dispersive micro-solid phase extraction of tetracyclines from human serum, Talanta 214 (2020), 120861, https://doi.org/10.1016/j.talanta.2020.120861.

[42] R.W. Silverstein, G.C. Bassler, Spectrometric identification of organic compounds, J. Chem. Educ. 39 (1962) 546–553, https://doi.org/10.1021/ed039p546.

[43] P. Makoś, A. Przyjazny, G. Boczkaj, Hydrophobic deep eutectic solvents as "green" extraction media for polycyclic aromatic hydrocarbons in aqueous samples, J. Chromatogr. A 1570 (2018) 28–37, https://doi.org/10.1016/j.chroma.2018.07.070.

[44] A. Pochivalov, K. Cherkashina, A. Shishov, A. Bulatov, Microextraction of sulfonamides from milk samples based on hydrophobic deep eutectic solvent formation by pH adjusting, J. Mol. Liq. 339 (2021), 116827, https://doi.org/10.1016/j.molliq.2021.116827.

[45] S. Dwivedi, J. Jadhav, H. Sharma, S. Biswas, Pulsed laser deposited ferromagnetic chromium dioxide thin films for applications in spintronics, Phys. Procedia 54 (2014) 62–69, https://doi.org/10.1016/j.phpro.2014.10.037.

[46] G.V. Chertihin, W.D. Bare, L. Andrews, Reactions of laser-ablated chromium atoms with dioxygen. Infrared spectra of CrO, OCrO, CrOO, CrO_3, $Cr(OO)_2$, Cr_2O_2, Cr_2O_3 and Cr_2O_4 in solid argon, J. Chem. Phys. 107 (1997) 2798–2806, https://doi.org/10.1063/1.474637.

[47] M. Gamal, I.A. Naguib, D.S. Panda, F.F. Abdallah, Comparative study of four greenness assessment tools for selection of greenest analytical method for assay of hyoscine: N -butyl bromide, Anal. Methods 13 (2021) 369–380, https://doi.org/10.1039/d0ay02169e.

[48] H.M. Mohamed, N.T. Lamie, Analytical eco-scale for assessing the greenness of a developed RP-HPLC method used for simultaneous analysis of combined antihypertensive medications, J. AOAC Int. 99 (2016) 1260–1265, https://doi.org/10.5740/jaoacint.16-0124.

[49] C.M. Teglia, F.A. Perez, N. Michlig, M.R. Repetti, H.C. Goicoechea, M.J. Culzoni, Occurrence, distribution, and ecological risk of fluoroquinolones in rivers and wastewaters, Environ. Toxicol. Chem. 38 (2019) 2305–2313, https://doi.org/10.1002/etc.4532.

[50] Q. Xue, C. Wang, Y. Lin, T.F. Jiang, Z. Lv, Determination of fluoroquinolones illegally added in traditional prostate medicines by ultrasonic-assisted dispersive liquid liquid micro-extraction based on deep eutectic solvent combined with quantitative 19F nuclear magnetic resonance method, Microchem. J. 170 (2021), 106725, https://doi.org/10.1016/j.microc.2021.106725.

[51] K. Yu, M.E. Yue, J. Xu, T.F. Jiang, Determination of fluoroquinolones in milk, honey and water samples by salting out-assisted dispersive liquid-liquid microextraction based on deep eutectic solvent combined with MECC, Food Chem. 332 (2020), 127371, https://doi.org/10.1016/j.foodchem.2020.127371.

[52] I. Timofeeva, K. Stepanova, A. Shishov, L. Nugbienyo, L. Moskvin, A. Bulatov, Fluoroquinolones extraction from meat samples based on deep eutectic solvent formation, J. Food Compos. Anal. 93 (2020), 103589, https://doi.org/10.1016/j.jfca.2020.103589.

[53] W. Ma, K.H. Row, Hydrophilic deep eutectic solvents modified phenolic resin as tailored adsorbent for the extraction and determination of levofloxacin and ciprofloxacin from milk, Anal. Bioanal. Chem. 413 (2021) 4329–4339, https://doi.org/10.1007/s00216-021-03389-2.